Journal of Engineering Research and Reports

Volume 26, Issue 6, Page 307-318, 2024; Article no.JERR.117156
ISSN: 2582-2926

Design and Kinematics Analysis of Tensioning Integral Robot

Shoubo Wang [a*] and Hongze Liu [a]

[a] North China University of Water Resources and Electric Power, Zhengzhou, Henan, China.

Authors' contributions

This work was carried out in collaboration between both authors. Both authors read and approved the final manuscript.

Article Information

DOI: https://doi.org/10.9734/jerr/2024/v26i61182

Open Peer Review History:
This journal follows the Advanced Open Peer Review policy. Identity of the Reviewers, Editor(s) and additional Reviewers, peer review comments, different versions of the manuscript, comments of the editors, etc are available here: https://www.sdiarticle5.com/review-history/117156

Opinion Article

Received: 20/03/2024
Accepted: 24/05/2024
Published: 29/05/2024

ABSTRACT

In the past two decades, the technology of robots has developed rapidly. With the enrichment of social needs and applications, the functions of robots have become diversified. The tension-integrated robot designed in this paper is based on the British OC Robotics Series II X125 robot for mechanism design. The mathematical model of the tension-integrated robot is derived, and the kinematic simulation is carried out by Adams and Matlab to verify the correctness of the mathematical model, and the kinematic analysis of the tension-integrated robot is carried out.

Firstly, the development and research status of tensioning integral robot is briefly summarized. Because the shape of the tensioning integral robot designed in this paper is similar to that of a snake, the development, structural characteristics and research status of the snake robot are summarized.

Secondly, according to the application requirements of the tensioned integral robot, the functions and performance indexes of the tensioned integral robot are analyzed, and the overall structure of the tensioned integral robot is designed, including the body structure of the snake robot, the driving mechanism and the base. The serpentine arm of the serpentine robot is a serpentine structure with twelve joints connected in series.

**Corresponding author: Email: 878604878@qq.com;*

Cite as: *Wang , Shoubo, and Hongze Liu. 2024. "Design and Kinematics Analysis of Tensioning Integral Robot". Journal of Engineering Research and Reports 26 (6):307-18. https://doi.org/10.9734/jerr/2024/v26i61182.*

Finally, the mathematical model of the snake robot is derived, and the kinematic simulation of the snake robot is carried out by Adams and Matlab respectively. The obtained image results are the same, which proves that the mathematical model of the snake robot is correctly derived, laying a foundation for further research.

Keywords: Snake robot; tensioning integral structure; kinematics modeling; Matlab; Adams.

1. INTRODUCTION

At present, many countries have carried out the exploration of the snake robot, because the snake robot can basically reach the corner of the human can not reach, such as the disaster area, underground mining, nuclear pollution areas and other complex environment; For the environment with many obstacles, uneven and narrow terrain, snake robots can play a greater advantage to meet the different needs of human beings. China's robot industry developed late, compared with some developed countries, the technology is not mature, but in recent decades, with the improvement of the national level of science and technology, the smooth development of the national high-tech research and development program, China in the space, underwater, nuclear fields and other special robots have achieved gratiling results, a number of robot products and robot application industry came into being. It is understood that the research and development of snake robot has covered robot system, artificial intelligence, robot mechanism, robot electrical, servo motor and other aspects, and has initially formed the ability of robot parts and whole machine research and development, and has the ability to produce and assemble and debug, and has the ability to establish a robot design and development platform [1].

This project designs and studies a tension-integrated robot, also known as a snake robot. Based on the Series II X125 robot of OC Robotics in the UK, this project designs a new overall configuration of a snake robot with similar parameters. The snake robot has a variety of motion forms and functions. Snake-like robots are also more economical and reliable. Tensioning integral robot is a kind of parallel robot, because the parallel mechanism has the advantages of large stiffness, small cumulative error, high control accuracy, strong bearing capacity, etc., it has been widely used in the fields of motion simulation, space docking, processing and manufacturing. Different from the traditional parallel mechanism, the tensioning integral parallel mechanism contains elastic components, and the use of elastic components makes this kind of mechanism have the ability of underdriving [14,15]. In addition, tensioning monolithic structures commonly used in the field of architecture have the characteristics of high strength-mass ratio, strong deformability, and compressive and seismic resistance, and can be applied to the design of mobile robots to produce lightweight disaster rescue robots that adapt to complex ground environments [2]. The overall shape of the tensioning integral robot is snake-like, and the rod members can be telescoped by ropes. This snake-like structure composition can make the volume of the structure itself in a small state, which is convenient for investigation and rescue. Therefore, the tensioned monolithic snake robot has the absolute advantage of becoming a probe robot.

2. RESEARCH STATUS OF TENSIONING INTEGRAL ROBOT AT HOME AND ABROAD

The algorithm reported by D. Permer [3] demonstrates a method for actively winding/unwinding continuous arms on a spiral drum, which can be used for multiple tracks in actual computational time with a deviation of less than 3 mm from the desired trajectory.Xu[4] proposed a method based on force density method to optimize the connection degree and node position of tensioning monolithic structures. The method has a general formula that can be reduced to a transformation form to find the formula. The effectiveness of the proposed method is verified by numerical examples, which show that not only the classical tensioning integral system but also the new tensioning integral system can be obtained by this method. Pettersen[5] established the mathematical model of a snake robot used for submarine inspection, carried out kinematic analysis, and designed the underwater swimming manipulator. Pettersen's team [6] completed the preliminary research work such as the modeling of the snake robot and challenged the snake robot to move in a more challenging environment.

Li Bingyu [7] from Dalian University of Technology studies flexible robots. First, he

designs the whole robot arm, then conducts kinematics and dynamics modeling for the tension-integrated continuous robot arm, and simulates it in Matlab. Finally, he builds an experimental platform to prove the correctness of the mechanical model. Ji Hongna [8] of Xidian University first carried out the dynamic model and motion analysis of the tensioned integral robot, then carried out the motion trajectory planning of the tensioned integral robot, and developed the motion simulation software of the tensioned integral robot.Chen Chaowei [9] from Xidian University studied the finite element model of the tensioned integral structure, conducted modal analysis of the tensioned integral structure, and conducted vibration test of the tensioned integral structure. Ji Zhifei [10] from Xidian University studied the 3-SPS tension-stretch integral parallel mechanism, and analyzed the position of the 3-SPS tension-stretch integral parallel mechanism, and obtained the inverse position solution and the positive position solution. In the end, the kinetics was studied. Zhao Zhiyuan [11] from the University of Chinese Academy of Sciences designed the mechanical system of the linear driven continuous robotic arm and designed its end capturing mechanism. The next step was the kinematic analysis of the linear driven continuous robotic arm, and finally the motion planning of the linear driven continuous robotic arm was carried out in a narrow space environment. Liu Tianliang [12] from Harbin Institute of Technology conducted research on the rope-driven super-redundant robotic arm, and designed the system of the rope-driven super-redundant robotic arm. In the next step, the kinematics analysis of the rope-driven super-redundant robotic arm was carried out, and finally the experimental research was conducted on the integration of the prototype of the rope-driven robotic arm. Yang Wenlong [13] from Harbin Institute of Technology studied the overall design of continuous robotic arm for single-hole endoscopic surgery, studied the mechanical model of the incisional continuous robotic arm, and modeled its kinematics.

3. MECHANISM DESIGN OF TENSIONING INTEGRAL ROBOT

3.1 Tensioning Integral Robot Design Requirements

Combining the design concept of flexible robot and the design characteristics of new snake robot, the 12-joint snake robot is designed in this paper. The design of the overall structure of tensioning integral robot is the key to the design of tensioning integral robot. The overall structure directly affects the performance indicators of the snake robot, and the snake robot also directly affects the design of the drive module and the selection of the motor. In the third chapter, the function requirements and performance indexes of the snake robot are proposed, the characteristics of each joint of the snake robot are analyzed, and the rope drive is determined. The snake robot adopts steel wire rope traction and universal joint design.

The tensioning integral robot designed in this paper needs to have the ability to cross the narrow space and enter the complex area for detection, maintenance and other work. Therefore, the overall function of the tensioning robot is required:

(1) The ability of traversing narrow space: First, the tensioning integral robot should have a large aspect ratio, which can meet the task of traversing narrow space in terms of structure size; Secondly, the tensioning integral robot should have more degrees of freedom, which can meet the requirements of flexibly avoiding obstacles.

(2) It can accomplish specific tasks: the tensioned integral robot end can carry a detector, which requires that the end of the robot arm can bear a certain weight.

(3) Sufficient motion accuracy and reliability and durability: the tensioning integral robot must ensure smooth movement, which requires sufficient stiffness and strength, and also needs to be able to work in harsh environments such as high temperature and high pressure.

3.2 Tensioning Integral Robot Drive Mode Selection

The driving mode of tensioning integral robot is the motion mode of bending the joints of the snake robot. The traditional robot uses a reducer to directly drive the joint rotation, which can not meet the needs of passing through the narrow space. The snake robot uses a rope to drive the joint for movement, and the drive motor and transmission structure are placed on the base of the snake robot tail. The snake-like robot has four advantages: first, it can transmit large power, and different driving ropes

Fig. 1. 3D diagram of a snake robot

can be selected according to different needs; Second, the rope drive of the snake robot is stable and reliable; Third, the driving rope can make the snake robot bend at a large Angle, and the driving rope is light in weight. Fourth, the same drive base can choose different drive ropes to control different snake robots.

3.3 Three-Dimensional Solid Modeling of Tensioned Integral Robot

The snake arm is the most important component of the snake robot. The joints connected by the snake robot should not only ensure stable connection, safety and reliability, but also ensure the flexibility of the snake robot and ensure normal movement at every Angle. When using 3D modeling software Solidworks to model the whole tensioning robot, each part should be guaranteed to be correct, so as to ensure that there will be no problems in later assembly. The final 3D drawing of the snake robot is shown in Fig. 1. Moreover, the later kinematic, dynamic and modal analysis work is carried out.

4. KINEMATIC ANALYSIS OF TENSIONING INTEGRAL ROBOT

The tensioning integral robot is formed through the series of tensioning integral units and driven by ropes. In this chapter, the relationship between drive space, joint space and operation space is established from the base coordinates, and the angular velocity and velocity of each joint of the snake robot are obtained. On this basis, the kinematics simulation of the snake robot is carried out, and the time curves of displacement and velocity are obtained by Matlab and Adams respectively, and the correctness of the derived mathematical model is verified.

4.1 Kinematic Modeling

The forward kinematics model from joint space to task space was established based on homogeneous coordinate transformation. S is the base coordinate system, G is the target coordinate system, B is the first joint coordinate system, W is the last joint coordinate system, the target coordinate system and the base coordinate system are fixed, the transformation relationship from S to G is ${}^{S}_{G}T$, the transformation relationship from S to B is ${}^{S}_{B}T$, and the transformation relationship of the snake arm is ${}^{B}_{W}T$. The rotating joint has two rotational degrees of freedom, and the establishment of the coordinate system should coincide with the center of the joint. The following is the kinematic model derivation of the snake robot:

$$ {}^{0}_{1}T = \begin{bmatrix} 1 & 0 & 0 & 0 \\ 0 & 1 & 0 & 0 \\ 0 & 0 & 1 & d_1 \\ 0 & 0 & 0 & 1 \end{bmatrix} \quad (1) $$

$$ {}^{1}_{2}T = \begin{bmatrix} s\theta_1 & c\theta_1 & 0 & 0 \\ 0 & 0 & 1 & 0 \\ c\theta_1 & -s\theta_1 & 0 & 0 \\ 0 & 0 & 0 & 1 \end{bmatrix} \quad (2) $$

$$ {}^{2}_{3}T = \begin{bmatrix} c\varphi_1 & s\varphi_1 & 0 & 0 \\ 0 & 0 & 1 & 0 \\ s\varphi_1 & c\varphi_1 & 0 & 0 \\ 0 & 0 & 0 & 1 \end{bmatrix} \quad (3) $$

$$ {}^{3}_{4}T = \begin{bmatrix} c\theta_2 & s\theta_2 & 0 & \ell_1 \\ 0 & 0 & -1 & 0 \\ s\theta_2 & c\theta_2 & 0 & 0 \\ 0 & 0 & 0 & 1 \end{bmatrix} \quad (4) $$

$$ {}^{4}_{5}T = \begin{bmatrix} c\varphi_2 & s\varphi_2 & 0 & 0 \\ 0 & 0 & 1 & 0 \\ s\varphi_2 & c\varphi_2 & 0 & 0 \\ 0 & 0 & 0 & 1 \end{bmatrix} \quad (5) $$

Formula 1 is the transformation matrix from the connection between the motor and the serpentine arm to the first joint, Formula 2 is the transformation matrix from the first joint to the second joint, formula 3 is the transformation matrix from the second joint to the third joint, Formula 4 is the transformation matrix from the third joint to the fourth joint, and formula 5 is the transformation matrix from the fourth joint to the fifth joint. Where s is $\sin$ the abbreviation of the above formula, c is $\cos$ the abbreviation.
Specific calculations are as follows:

$$ {}^{1}_{3}T\left(\theta_1\varphi_1\right) = {}^{1}_{2}T \cdot {}^{2}_{3}T = \begin{bmatrix} s\theta_1 c\varphi_1 & -s\theta_1 s\varphi_1 & c\theta_1 & 0 \\ -s\varphi_1 & -c\varphi_1 & 0 & 0 \\ c\theta_1 c\varphi_1 & -c\theta_1 s\varphi_1 & -s\theta_1 & 0 \\ 0 & 0 & 0 & 1 \end{bmatrix} \quad (6) $$

Formulas 6 are the product of the transformation matrix from the first joint to the second joint and the transformation matrix from the second joint to the third joint.
Then calculate according to (6) to get the general formula:

$$ {}^{2i-1}_{2i+1}T(\theta_i, \varphi_i) = {}^{2i-1}_{2i}T\ {}^{2i}_{2i+1}T = \begin{bmatrix} c\theta_i c\varphi_i & -c\theta_i s\varphi_i & -s\theta_i & l_{i-1} \\ s\varphi_i & c\varphi_i & 0 & 0 \\ s\theta_i\varphi_i & -s\theta_i s\varphi_i & c\theta_i & 0 \\ 0 & 0 & 0 & 1 \end{bmatrix} \quad (7) $$

$$ {}^{B}_{W}T = \prod_{i=0}^{12} Ti \quad (8) $$

Formula 8 is the form of the transformation matrix from the 1st joint to the 12th joint.

$$ T_i = \begin{bmatrix} R_i & P_i \\ 0 & 1 \end{bmatrix} \quad i = 0,1,2,\cdots 12 \quad (9) $$

Where i=0, formula 10 and formula 11 can be obtained:

$$R_i = \begin{bmatrix} 1 & 0 & 0 \\ 0 & 1 & 0 \\ 0 & 0 & 1 \end{bmatrix} = {}_1^0 R \qquad (10)$$

Formula 10 represents the attitude from the initial point of the serpentine arm to the first joint.

$$p_i = \begin{bmatrix} 0 \\ 0 \\ di \end{bmatrix} \qquad (11)$$

Formula 11 represents the position from the initial point of the serpentine arm to the first joint. i=1:

$$R_i = \begin{bmatrix} s\theta_i c\varphi_i & -s\theta_i s\varphi_i & c\theta_i \\ -s\varphi_i & -c\varphi_i & 0 \\ c\theta_i c\varphi_i & -c\theta_i s\varphi_i & -s\theta_i \end{bmatrix} \qquad (12)$$

Formula 12 represents the pose from the first joint to the second joint.

$$p_i = \begin{bmatrix} 0 \\ 0 \\ 0 \end{bmatrix} \qquad (13)$$

Formula 13 represents the position of the first joint to the second joint.

$i = 2,3,4 \cdots 12$

$$R_i = \begin{bmatrix} c\theta_i c\varphi_i & -c\theta_i s\varphi_i & -s\theta_i \\ s\varphi_i & c\varphi_i & 0 \\ s\theta_i c\varphi_i & -s\theta_i s\varphi_i & c\theta_i \end{bmatrix} = {}_{2i+1}^{2i-1} R \qquad (14)$$

Formula 14 represents the pose from the second joint to the twelfth joint.

$$\boldsymbol{P_i} = \begin{bmatrix} \boldsymbol{l_{i-1}} \\ \mathbf{O} \\ \mathbf{O} \end{bmatrix} \qquad (15)$$

Formula 15 represents the position of the second joint through the twelfth joint.

Therefore, according to the above formula ${}_{\omega}^{\mathrm{B}}T$ can be written in the following form:

$${}_{\omega}^{B}T = \prod_{i=0}^{12} T_i = \prod_{i=0}^{12} \begin{bmatrix} R_i & P_i \\ 0 & 1 \end{bmatrix} \qquad (16)$$

$$= \begin{bmatrix} \prod_{i=0}^{12} R_i & P_0 + \sum_{i=1}^{12} \left(\left(\prod_{j=0}^{i=1} R_j \right) R_i \right) \\ 0 & 1 \end{bmatrix} \qquad (17)$$

$${}_{\omega}^{B}T = \prod_{i=0}^{12} T_i = \prod_{i=0}^{12} \begin{bmatrix} R_i & P_i \\ 0 & 1 \end{bmatrix} \qquad (18)$$

$${}_{\omega}^{B}T = \begin{bmatrix} {}_{25}^{0}R & P_0 + \sum_{i=1}^{12} {}_{2i-1}^{0} R P_i \\ 0 & 1 \end{bmatrix} \qquad (19)$$

The above formula 19 is split into position and attitude.

$${}^{B}P = P_0 + \sum_{i=1}^{12} {}_{2i-1}^{0} R_i P_i \qquad (20)$$

Formula 20 above is the position expression of the snake robot.

$${}_{\omega}^{B}\boldsymbol{R} = {}_{25}^{0}\boldsymbol{R} \qquad (21)$$

Formula 21 is the attitude expression of a snake robot.

The most direct way to find the linear velocity in the base coordinate system of a snake robot is to differentiate it by definition.

$${}^{B}P = P_0 + \sum_{i=2}^{12} |_{i-1} \hat{X}_{2i-1} \qquad (22)$$

Taking the time derivative of equation 15 gives equation 23.

$${}^{B}\boldsymbol{V}_{w} = \frac{d\,{}^{B}\boldsymbol{P}_{w}}{d_t} = \boldsymbol{P}_0 + \sum_{i=2}^{12} l_{i-1}\, \hat{X}_{2i-1} \qquad (23)$$

${}_{B}^{A}R$ rotation matrix is shown in equation 24.

$${}_{B}^{A}R = \begin{bmatrix} r_{11} & r_{12} & r_{13} \\ r_{21} & r_{22} & r_{23} \\ r_{31} & r_{32} & r_{33} \end{bmatrix} \qquad (24)$$

The formula of angular velocity and velocity of the serpentine arm is deduced by D-H method:

$$ {}^{1}w_1 = \begin{bmatrix} 0 \\ 0 \\ 0 \end{bmatrix} \tag{25} $$

$$ {}^{1}V_1 = \begin{bmatrix} 0 \\ 0 \\ d_1 \end{bmatrix} \tag{26} $$

$$ {}^{2}W_2 = {}^{2}_{1}R\,{}^{1}w_1 + \dot{\theta}_1\,{}^{2}\hat{z}_2 = \dot{\theta}_1\,{}^{2}\hat{z}_2\;{}^{2}V_2 = {}^{2}_{1}R({}^{1}v_1 + {}^{1}w_1 x' p_{20RG}) = {}^{2}_{1}R'v_1 \tag{27} $$

$$ {}^{3}W_3 = {}^{3}_{2}R\,{}^{2}w_2 + \dot{\psi}_1\,{}^{3}\hat{z}_3 = {}^{3}_{2}R\dot{\theta}_1^{2}\hat{z}_2 + \dot{\varphi}_1^{3}\hat{z}_3 \tag{28} $$

$$ {}^{3}V_3 = {}^{3}_{2}R\left({}^{2}V_2 + {}^{2}w_2 X\,{}^{2}P_{30RG}\right) = {}^{3}_{1}R\,{}^{1}V_1 \tag{29} $$

$$ {}^{4}W_4 = {}^{4}_{3}R\,{}^{3}w_3 + \dot{\theta}_2\,{}^{4}\hat{z}_4 = {}^{4}_{2}R\dot{\theta}_1^{2}\hat{z}_2 + {}^{4}_{3}R\dot{\varphi}_1\hat{z}_3 + \dot{\theta}_2^{4}\hat{z}_4 \tag{30} $$

$$ {}^{4}V_4 = {}^{4}_{3}R\left({}^{3}V_3 + {}^{3}w_3 \times {}^{3}P_{40RG}\right) = {}^{4}_{1}R'v_1 + {}^{4}_{3}R\,{}^{3}w_3 \times {}^{4}_{3}R_2 P_2 \tag{31} $$

$$ {}^{5}W_5 = {}^{5}_{4}R\,{}^{4}w_4 + \dot{\varphi}_2\,{}^{5}\hat{z}_5 = {}^{5}_{2}R\dot{\theta}_1^{2}\hat{z}_2 + {}^{5}_{3}R\dot{\varphi}_1\hat{z}_3 + {}^{5}_{4}R\,\dot{\theta}_2\,\hat{z}_4 + \dot{\varphi}_2^{5}\hat{z}_5 \tag{32} $$

$$ {}^{5}V_5 = {}^{5}_{4}R\left({}^{4}V_4 + {}^{4}w_4 \times {}^{4}P_{50RG}\right) = {}^{5}_{1}R\,{}^{1}V_1 + {}^{5}_{3}R\,{}^{3}w_3 \times {}^{5}_{3}RP_2 \tag{33} $$

The structural volume of the snake arm is summarized by equations 25, 26, 27, 28, 29, 30, 31, 32 and 33, which are summarized as follows:

$$ W_{2i+1} = \sum_{j=1}^{i} {}_{2j}R\dot{\theta}_j^{2j}\hat{z}_{2j} + \sum_{j=1}^{i} {}^{0}_{2j+1}R\dot{\varphi}_j^{2j+1}\hat{z}_{2j+1} \tag{34} $$

$$ V_{2i+1} = {}^{1}V_1 + \sum_{j=2}^{i} w_{2j-1} \times {}^{0}_{2j-1}RP_j \tag{35} $$

4.2 Adams Simulation

In this section, Adams tensioning integral robot 3D model will be used for kinematic analysis, and the data obtained by Matlab will be compared in the next section to verify the correctness of its mathematical model. SolidWorks 3D modeling software is used to establish the 3D model of the tension-whole robot, which is imported into Adams software, and the motion subconstraints are added between the relative moving parts and the drivers are added in the relevant parts, which is used to establish the motion simulation of the snake robot. Fig. 2 shows the snake robot model after adding motion pairs. Because the snake robot model contains a large number of parts, each independent moving component is taken out separately in SolidWorks and imported into Adams in the form of parts, which not only saves time, but also reduces the error rate.

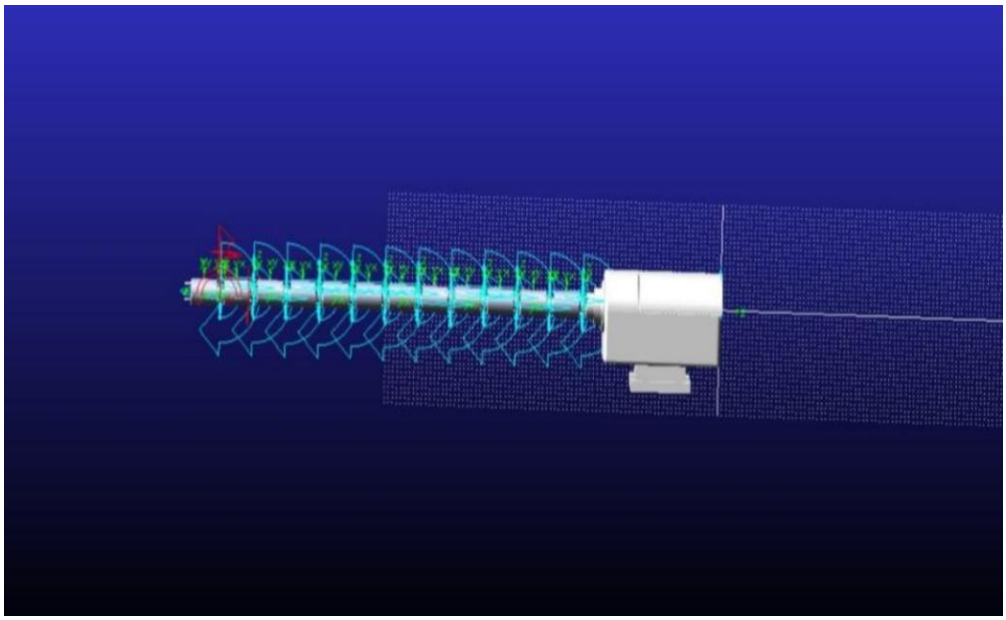

Fig. 2. Kinematic subconstraint

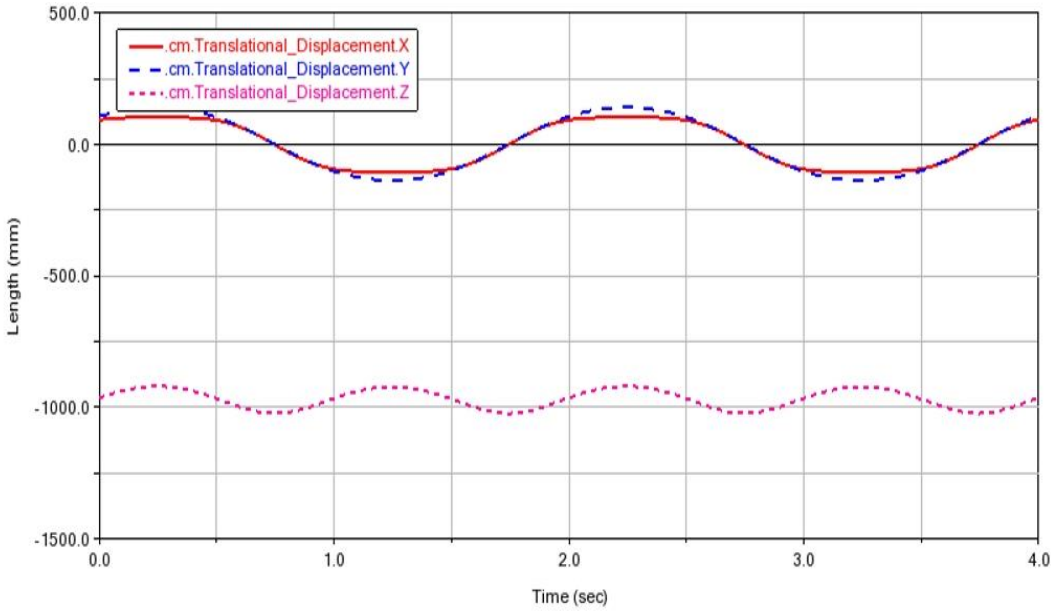

Fig. 3. Adams displacement and time curve

After the kinematics simulation of the snake robot is completed, the post processing module in 3D simulation software Adams will be used to analyze the motion of the snake robot, including the displacement and time curve and the speed and time curve, as shown in Fig. 3 and 4.

Displacement and time diagram of the snake robot: the curve X, Y and Z all show periodic changes. Through the analysis of the three curves, the ordinate is the displacement, the abscissa is the curve time is 4s, and the difference between the maximum value of the ordinate and the minimum value of the ordinate is the displacement of the drawn image. Because the moving image drawn is a straight line, the displacement in the three directions is a periodic curve.

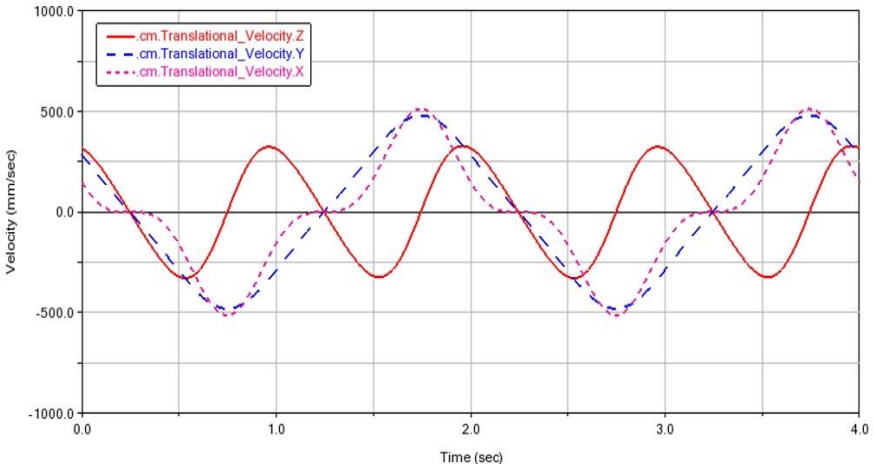

Fig. 4. Adams velocity and time curve

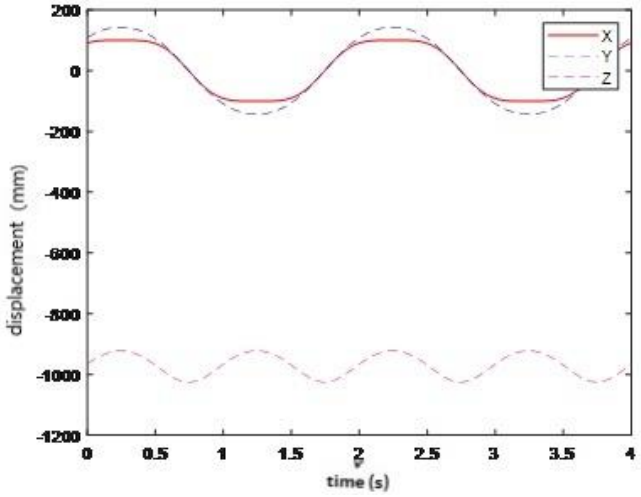

Fig. 5. Matlab reference point displacement curve

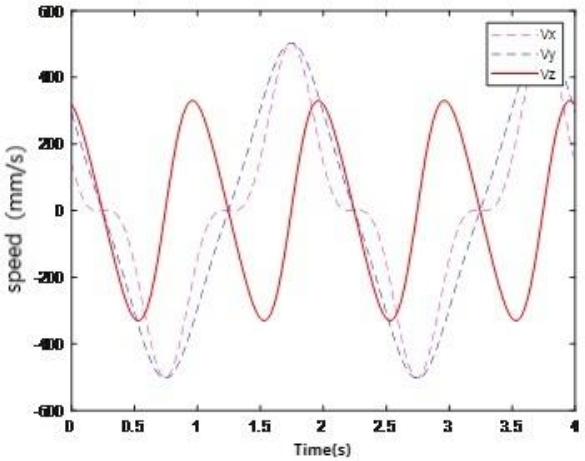

Fig. 6. Matlab reference point velocity curve

Velocity and time diagram of the snake robot: The curve X, Y and Z all show a cyclical change law. The X direction peaks when it approaches 1s, 2s, 3s and 4s, and peaks when it exceeds 0.5s, 1.5s, 2.5s and 3.5s. The Y direction has a peak value from 1.5s to 2s, a peak value from 3.5s to 4s, a trough value from 0.5s to 1s, and a trough value from 2.5s to 3s. The velocity in the Z direction peaks from 1.5s to 2s, peaks from 3.5s to 4s, troughs from 0.5s to 1s, and troughs from 2.5s to 3s. Through the analysis of the three curves of the velocity, the curve movement time is 4s, because the drawing image is a straight line, so the X, Y and Z direction velocity are periodic changes.

4.3 Matlab Simulation Calculation

The derived mathematical model is imported into Matlab for calculation and compared with the simulation results in Adams. The most important step in Matlab is to write the function according to the mathematical model. See the appendix for its writing content. t in the writing content represents the time, and fai(i-1,m) represents the i-1 row and m column in the fai matrix. Finally, the image results are obtained in Matlab, as shown in Fig. 5 and 6.

The above two images obtained by Matlab are compared with those obtained by Adams. It is found that the displacement components of X, Y and Z are basically the same, and there is no large deviation. By analyzing the velocity components of X, Y and Z, the image results obtained by Matlab are basically consistent with those obtained by Adams, and there is no large error. Through the above analysis, the correctness of the mathematical model derivation of the tensioned integral robot can be generally verified, which provides a basis for the feasibility of the following work.

The most important result of this chapter is the comparison between the image results obtained by Adams kinematics simulation and the image results obtained by Matlab calculation. The image comparison is basically the same, so the correctness of the mathematical model derivation can be verified.

5. CONCLUSION

In this paper, the development history and research status of tension-integrated robots at home and abroad are reviewed. The snake-shaped robot is taken as the research object, the position-forward and position-reverse solutions are studied, its structure is modeled by three-dimensional modeling software, and the correctness of position solution is verified by Adams software. The main research contents are as follows:

(1) For the tensioning integral robot mechanism studied, this paper first analyzes the structure and motion characteristics of the mechanism.

(2) Since the tensioning integral robot directly analyzes it and its complexity, this paper deduces the mathematical model of the tensioning integral robot by using D-H parameter method. Matlab software was used to solve and calculate the above mathematical model, and Solidworks 3D modeling software was used to model the whole tensioner robot. The model was processed and imported into Adams for kinematic simulation, and the simulation results based on mathematical model were compared and verified.

COMPETING INTERESTS

Authors have declared that no competing interests exist.

REFERENCES

1. Wang Yu, Anyou. Development History and Application Prospect Analysis of Snake Robot [J]. China Equipment Engineering, 2019;11:35-36
2. Sriram K, Anirudh K, Jayanth B, Anjaneyulu J. Design and kinematics analysis of suspension system for a formula society of automotive engineers (FSAE) Car. Journal of Engineering Research and Reports, 2021;21(2):48–63. Available:https://doi.org/10.9734/jerr/2021/v21i217445
3. Smith PN, Refshauge KM, Scarvell JM. Development of the concepts of knee kinematics. Archives of physical medicine and rehabilitation. 2003;84(12):1895-902.
4. Nagase K, Skelton RE. Network and vector forms of tensegrity system dynamics[J]. Mechanics Research Communications, 2014;59:14 to 25.
5. Palmer D; Axinte D.Active uncoiling and feeding of a continuum arm robot[J]. Robotics and Computer Integrated Manufacturing. 2019;56:107-116

6. Xu Kai; Liu Zenghui; Zhao Bin etc. Finding member connectivities and nodal positions of tensegrity structures based on force density method and mixed integer nonlinear programming[J] Mechanism and Machine Theory. 2018;166:240-250.
7. Pettersen Kristin Y. Snake Robot [J]Annual Reviews in Control. 2017;44:19-44
8. Pettersen Kristin YA review on modelling, implementation, and control of snake robots[J]Robotics and Autonomous Systems. 2012;1:29-40.
9. Li Bingyu. Design and research of continuous robotic arm based on tensioned integral structure [D]. Dalian University of Technology; 2020.
10. Hongna Ji. Dynamics and kinematic performance analysis of tensioned monolithic mobile robot [D]. Xidian University; 2011
11. Chen Chaowei. Optimal vibration control and actuator configuration of flexible tensioned monolithic structures [D]. Xidian University; 2012.
12. Zhifei JI. Configuration synthesis, kinematic performance analysis and energy harvesting of 3-sps tensioning monolithic parallel mechanism [D]. Xidian University; 2014.
13. Zhao Zhiyuan. Research on kinematics and motion planning of linear driven continuous manipulator [D]. University of Chinese Academy of Sciences (Changchun Institute of Optics, Fine Mechanics and Physics, Chinese Academy of Sciences); 2019.
14. Liu Tianliang. Research on wire-driven super-redundant robotic arm for small space operation [D]. Harbin Institute of Technology; 2016.
15. Yang Wenlong. Research oncontinuous robotic arm and its motion modeling for single-hole endoscopic surgery [D], Harbin Institute of Technology; 2016.

APPENDIX

```
clear
clc
% syms t
i=2;
l=825;%控制器长度
d=200;%杆 1-12 的各杆长度
A0=[1 0 0 0;0 1 0 0;0 0 1 -l;0 0 0 1];%0-1 的转换矩阵 A0
D=[1 0 0 0;0 1 0 0;0 0 1 -d;0 0 0 1];%
for t=0:0.01:4
for m=1:12
fai(i-1,m)=0.8*sin(pi*t+0.8*m);%输入
seita(i-1,m)=0.8*sin(pi*t+0.8*m);%输入
X{m}=[1 0 0 0
0 cos(seita(i-1,m)) -sin(seita(i-1,m)) 0
0 sin(seita(i-1,m)) cos(seita(i-1,m)) 0
0 0 0 1];
Y{m}=[cos(fai(i-1,m)) 0 sin(fai(i-1,m)) 0
0 1 0 0
-sin(fai(i-1,m)) 0 cos(fai(i-1,m)) 0
0 0 0 1];
A{m}=Y{m}*X{m}*D;%各矩阵通式
end
T=A0*A{1};
x(i,1)=-T(1,4);y(i,1)=T(2,4);z(i,1)=T(3,4);
i=i+1;
end
tt=0:0.01:4;
for n=1:401
Vx(n)=d*(0.8*pi*cos(pi*tt(n)+0.8))*(2*(cos(0.8*sin(pi*tt(n)+0.8)))^2-1);
Vy(n)=d*cos(0.8*sin(pi*tt(n)+0.8))*pi*0.8*cos(pi*tt(n)+0.8);
Vz(n)=d*(2*cos(0.8*sin(pi*tt(n)+0.8))*sin(0.8*sin(pi*tt(n)+0.8))*0.8*pi*cos(pi*tt(n)+0.8));
end
figure(1)

plot(tt,x(2:402,1),'-.',tt,y(2:402,1),'--',tt,z(2:402,1),'-')
title('参考点位移分量变化');
xlabel('时间(s)');ylabel('位移(mm)')
legend('X','Y','Z');

figure(2)
plot(tt,Vx(1,:),'-.',tt,Vy(1,:),'--',tt,Vz(1,:),'-')
title('参考点速度分量变化');
xlabel('时间(s)');ylabel('速度(mm/s)')
legend('Vx','Vy','Vz');
```


Peer-review history:
The peer review history for this paper can be accessed here:
https://www.sdiarticle5.com/review-history/117156